Disorder and interactions in quantum Hall ferromagnets near $\nu=1$

Jairo Sinova,[1,2] A. H. MacDonald,[2] and S. M. Girvin[2]
[1]*Department of Physics and Astronomy, University of Tennessee, Knoxville, Tennessee 37996*
[2]*Department of Physics, Indiana University, Bloomington, Indiana 47405*
(Received 19 April 2000)

We report on a finite-size Hartree-Fock study of the competition between disorder and interactions in a two-dimensional electron gas near Landau-level filling factor $\nu=1$. The ground state at $\nu=1$ evolves with increasing disorder from a fully spin-polarized ferromagnet with a charge gap to a partially spin-polarized ferromagnetic Anderson insulator, to a quasimetallic paramagnet at the critical point between $i=0$ and $i=2$ quantum Hall plateaus. Away from $\nu=1$, the ground state evolves from a ferromagnetic Skyrmion quasiparticle glass to a conventional quasiparticle glass, and finally to a conventional Anderson insulator. We comment on signatures of these different regimes in low-temperature transport and NMR line shape and peak position data.

I. INTRODUCTION

Because of the macroscopic degeneracy of single-particle states in a Landau level, neither disorder nor electron-electron interactions in a two-dimensional electron system (2DES) can be treated perturbatively in the quantum Hall regime. This is the raison d'être for the many interesting and surprising phenomena[1] which have arisen in quantum Hall physics. Theories of quantum Hall physics usually include either only interactions or only disorder, although both are always present. In particular, it is common to include only disorder in studies of the integer quantum Hall effect (IQHE), which generally focus on the sudden jump in the Hall conductivity between values separated by e^2/h, and it is common to include only interactions in studies of the fractional quantum Hall effect (FQHE), which generally focus on the ability of interactions to create charge gaps at partial Landau-level fillings. The competition between interactions and disorder has often, but not always,[2,3] been neglected, in part because of the lack of easily manageable analytical and numerical tools that can deal with both simultaneously. In this paper we address an instance in which this competition is particularly direct and can be successfully addressed with elementary techniques.

At Landau-level filling factor $\nu=1$, the ground state of a disorder-free 2DES is a strong ferromagnet,[4] i.e., it is completely spin polarized by a Zeeman field of infinitesimal strength. In practice, of course, the field experienced by a 2DES in the quantum Hall regime is *not* infinitesimal; however, the field's Zeeman coupling to the electron spin is typically very weak compared to other energy scales. (In referring to these systems as ferromagnets, we are emphasizing that they remain spin polarized in the limit of zero Zeeman splitting. In experimental systems,[5] typical values of the interaction and Zeeman energy scales are $\sim$160 K and $\sim$3 K respectively. The spin splitting produced by this bare Zeeman coupling is usually negligible in paramagnetic states.) The quantum Hall ferromagnet has a large gap for charge excitations, and hence has a robust quantum Hall effect. For typical Zeeman coupling strengths, its elementary charged excitations are topologically charged spin textures (Skyrmions) containing several flipped spins.[1,4,6] Large Skyrmions have a Hartree energy cost smaller that those of conventional quasiparticles and, because the spins align locally, only slightly higher exchange energy.[7] Because Skyrmions are the lowest-energy charged excitations, the global electron spin polarization is expected to decrease rapidly as $|1-\nu|$ increases. This has been observed in nuclear magnetic resonance (NMR) experiments.[1,5,6] On the other hand, the $\nu=1$ state of noninteracting disordered electrons differs qualitatively. The ground state is a compressible paramagnet with no Knight shift and no gap for charged excitations. For zero Zeeman coupling, quasiparticle states at the Fermi energy are quasiextended and cause the Hall conductivity to suddenly jump by $2e^2/h$ as this filling factor is crossed; $\nu=1$ is in the middle of a Hall ''riser,'' instead of being at the middle of a Hall plateau.

The competition between disorder and interactions at $\nu=1$ can be addressed[8] using the Hartree-Fock approximation, which has the virtue of being exact[1] in both the noninteracting and the nondisordered limits. Experimental information on this competition comes primarily from transport and NMR studies. Early NMR studies[5] of weak-disorder quantum Hall ferromagnets yielded relatively featureless line shapes and Knight shifts in good agreement with Hartree-Fock (HF) theory estimates[6,7,9] of Zeeman-coupling and filling-factor-dependent Skyrmion sizes. (Effective field theory estimates[4,10] are not accurate in the case of typical Zeeman coupling strengths.) More recent experiments[11] paint a more complex picture, in part because the measurements were performed at lower temperatures where the signal is not motionally averaged.[12,13] It is now clear that disorder plays a role in the interpretation of these experiments, even when it is weak. At stronger disorder, as the noninteracting limit is approached, the spin polarization must eventually vanish. In our model calculations we find that as the interaction strength is increased relative to disorder at $\nu=1$, the 2DES ground state suffers a continuous phase transition from a paramagnetic to a ferromagnetic state. Depending on the details of the disorder model, a second continuous phase transition to a fully spin-polarized incompressible strong ferromagnet with a gap for charged excitations may occur at

still stronger interactions. For the disorder models we use, the fully polarized state is reached when the Coulomb energy scale is approximately twice the Landau-level-broadening disorder energy scale. Away from $\nu=1$, screening by mobile charges reduces the importance of disorder and the system reaches maximal spin polarization at smaller interaction strengths. The maximally polarized ground state at moderate interaction strengths is best described as a glass of localized conventional quasiparticles formed in the $\nu=1$ fully polarized vacuum. Only for stronger interactions do we find a phase transition to a state with noncollinear magnetization in which the localized particles have Skyrmionic character.

We organize this paper as follows. In Sec. II we summarize our implementation of finite-size HF theory in the lowest Landau level (LLL). In Secs. III and IV we present and discuss our numerical results for calculations at $\nu=1$ and $\nu\neq1$. The possibility, discussed in recent work,[3] that at $\nu=1$ disorder will induce reduced-size Skyrmion–anti-Skyrmion pairs in the ground state is specifically addressed in Sec. III. Finally, in Sec. V we present our conclusions.

II. HARTREE-FOCK THEORY IN THE LLL

The HF approximation allows the interplay between disorder and interactions to be addressed while retaining a simple independent-particle picture of the many-body ground state. For the current study, the use of this approximation is underpinned by the fact that it reproduces the exact ground state at $\nu=1$ in both weak interaction and strong interaction[1] limits. HF theory is a self-consistent mean-field theory, and as such it has strengths and shortcomings, which we discuss later. In this section, we outline the basic formalism of HF approximation calculations in the LLL limit.

In a strong magnetic field, the Landau-level splitting is very large and, since excitations to higher Landau levels are effectively forbidden at the low experimental temperatures, we follow the common practice of considering only LLL states. This neglecting of Landau-level mixing allows us to ignore such effects as levitation of critical states, which could have an important effect in low magnetic fields.[14] Neglecting the frozen kinetic-energy degree of freedom, the Hamiltonian in second quantization is written as

$$\mathcal{H}=\mathcal{H}_I+\mathcal{H}_{\rm dis}+\mathcal{H}_Z, \tag{1}$$

where $\mathcal{H}_I$ is the interaction part of the Hamiltonian,

$$\mathcal{H}_I=\frac{1}{2}\int d\mathbf{r}\int d\mathbf{r}'\sum_{\sigma\sigma'} v_I(\mathbf{r}-\mathbf{r}') \times\hat{\psi}^\dagger_\sigma(\mathbf{r})\hat{\psi}^\dagger_{\sigma'}(\mathbf{r}')\hat{\psi}_{\sigma'}(\mathbf{r}')\hat{\psi}_\sigma(\mathbf{r}),$$

$\mathcal{H}_{\rm dis}$ is the external disorder part of the Hamiltonian,

$$\mathcal{H}_{\rm dis}=\int d\mathbf{r}\sum_\sigma v_E(\mathbf{r})\hat{\psi}^\dagger_\sigma(\mathbf{r})\hat{\psi}_\sigma(\mathbf{r}),$$

and $\mathcal{H}_Z$ is the Zeeman term,

$$\mathcal{H}_Z=-\frac{1}{2}g\mu_B\int d\mathbf{r}\sum_{\sigma\sigma'}\hat{\psi}^\dagger_{\sigma'}(\mathbf{r}')\hat{\psi}_\sigma(\mathbf{r}')\vec{\tau}_{\sigma'\sigma}\cdot\vec{B}(\vec{r}),$$

with $\sigma=\uparrow,\downarrow$, v_I and v_E being the Coulomb interaction and disorder potentials, respectively, and τ_i being the Pauli matrices. Here we also define the Zeeman coupling strength as $\tilde{g}=g\mu_BB/(e^2/\epsilon l)$ for later reference. We chose the Landau gauge elliptic theta functions as our basis,

$$\phi_m(x,y)=\frac{1}{\sqrt{L_y l\sqrt{\pi}}}\sum_{s=-\infty}^{\infty}e^{i(1/l^2)x_{m,s}y}e^{-(1/2l^2)(x-x_{m,s})^2},$$

where $x_{m,s}=(2\pi ml^2/L_y)+sL_x$, $m,m'=1,\ldots,N_\phi$, $N_\phi=A/(2\pi l^2)$, and l is the magnetic length which we set equal to 1 for simplicity. These wave functions satisfy the semiperiodic boundary conditions $\phi_m(x,y)=\phi_m(x,y+L_y)$ and $\phi_m(x+L_x)=\exp(+iL_xy/l^2)\phi_m(x,y)$.

We consider the HF single-particle states to be a linear combination of the up and down spin states of these basis functions,

$$|\alpha\rangle=\sum_{m,\sigma}\langle m\sigma|\alpha\rangle|m\sigma\rangle.$$

Before writing down the Hamiltonian matrix in the HF approximation, we introduce several notation-simplifying definitions, closely following previous HF studies.[8] The expectation value of the particle density (in momentum space) is given by

$$\langle\rho(\mathbf{q})\rangle=\sum_\alpha n_F(\epsilon_F-\epsilon_\alpha)\langle\alpha|e^{-i\mathbf{q}\cdot\mathbf{r}}|\alpha\rangle \equiv N_\phi e^{-(1/4)q^2}\sum_{\sigma,\sigma'}\delta_{\sigma,\sigma'}\Delta_{\sigma'\sigma}(\mathbf{q})e^{-i(q_xq_y/2)},$$

where we define

$$\Delta_{\sigma'\sigma}(\mathbf{q})\equiv\frac{1}{N_\phi}\sum_{m,m'}\delta_{(x_{m'},x_m+q_y)}e^{-iq_xx_m}\rho_{\sigma'\sigma}(x_{m'}|x_m)$$

and

$$\rho_{\sigma'\sigma}(x_{m'}|x_m)=\sum_\alpha n_F(\epsilon_F-\epsilon_\alpha)\langle m'\sigma'|\alpha\rangle\langle\alpha|m\sigma\rangle.$$

Here $\delta_{(x_{m'},x_m+q_y)}$ is a periodic Kronig delta function, i.e., it is nonzero for $x_{m'}=x_m+q_y+sL_x$ for any integer s. With these definitions we can write the Hamiltonian matrix in the HF approximation in a compact form that is simple to diagonalize numerically,

$$\langle m\sigma|\mathcal{H}|m'\sigma'\rangle_{\rm HF}=\sum_{\mathbf{q}\in{\rm BZ}}\Big\{[\gamma\Delta_0(\mathbf{q})U_H(\mathbf{q})+U_{\rm dis}(\mathbf{q})]I +\frac{\gamma}{2}[\Delta_0(\mathbf{q})I+\vec{\Delta}(\mathbf{q})\cdot\vec{\tau}]U_F(\mathbf{q})\Big\} \times\delta_{(x_m,x_{m'}+q_y)}e^{+iq_xx_{m'}}-\frac{1}{2}\tilde{g}\hat{B}\cdot\vec{\tau}, \tag{2}$$

where $\Delta_\alpha(\mathbf{q})={\rm Tr}\{\Delta_{\sigma\sigma'}(\mathbf{q})\tau^\alpha\}$, $\hat{B}$ specifies the orientation of the external magnetic field, and I is the identity matrix. The various effective potentials which appear here are defined as

$$U_{\rm dis}(\mathbf{q})=\frac{1}{A}\sum_{\mathbf{G}} e^{-(1/4)|\mathbf{q}+\mathbf{G}|^2} v_E(\mathbf{q}+\mathbf{G}) e^{(i/2)(q_x+G_x)(q_y+G_y)}, \tag{3}$$

$$U_H(\mathbf{q})=\frac{1}{2\pi}\sum_{\mathbf{G}} e^{-(1/2)|\mathbf{q}+\mathbf{G}|^2}\frac{2\pi e^2}{|\mathbf{q}+\mathbf{G}|}(1-\delta_{\mathbf{q}+\mathbf{G},0}), \tag{4}$$

and

$$U_F(\mathbf{q})=-\frac{1}{A}\sum_{\mathbf{q}'} e^{-(1/2)|\mathbf{q}'|^2} e^{iq_x' q_y - iq_x q_y'}\frac{2\pi e^2}{|\mathbf{q}'|}(1-\delta_{\mathbf{q}',0}), \tag{5}$$

with $\mathbf{G}=((2\pi N_\phi/L_x)n_x,(2\pi N_\phi/L_y)n_y)$.

For $v_E(\mathbf{r})$, we choose a white noise potential without spatial correlation, $\langle\langle v_E(\mathbf{r})v_E(\mathbf{r}')\rangle\rangle=\sigma^2\delta(\mathbf{r}-\mathbf{r}')$. The density of states in the noninteracting limit has been calculated exactly by Wegner for this distribution of the disorder potential,[15] yielding a full width at half maximum of approximately 1.06σ. In our calculations the parameter $\gamma=e^2/\epsilon\sigma$ specifies the relative strength of interactions and disorder broadening. This type of disorder potential distribution is characterized by a single parameter σ, which we use as our unit of energy. As we discuss later, our results are insensitive to correlations in the disorder potential on length scales smaller than l, but would change in some respects for disorder potentials which are smooth on the magnetic length scale.

The HF equations are solved by an iterative approach which can create difficulties which must be addressed. The HF equations generally have many solutions that correspond to different, usually metastable, extrema of the HF energy functional. The challenge is to locate the true global minimum. In particular, the iteration process will not break any symmetries of the Hamiltonian which are not broken by the starting charge and spin densities, even though the global minimum of the HF energy functional frequently does break at least some of these symmetries. To counter such problems, it is usually a good idea to introduce small artificial terms in the Hamiltonian which break the continuous symmetries and help the iterative process to reach the lowest-energy state. In this problem, the iterative process is also hampered by severe convergence problems at zero temperature connected with the localization of HF quasiparticle wave functions and the long-range nature of the Coulomb interactions. A small change in the energy of a particular orbital may involve a substantial rearrangement of the charges. These problems can be mitigated by always working at a temperature which is comparable to the finite-size quasiparticle energy level spacing and which scales to zero as the system size increases. The Zeeman term in the Hamiltonian, for which we choose typical experimental values, reduces the SU(2) spin symmetry to a U(1) symmetry. In order to break the continuous U(1) symmetry, we introduce an artificial (but very small) local magnetic field at the center of our simulation cells which points in the x direction. It is this space-dependent field, required on purely technical grounds, which has motivated developing the formalism in a manner which permits nonconstant Zeeman coupling strengths. To ensure that this artificial field and the finite temperature do not affect the final solution, we lower the magnitude of these terms until no change is seen in local charge and spin densities, or in HF quasiparticle energies.

The phase diagrams discussed in Secs. III and IV were obtained by starting from the noninteracting case and incrementing the interaction strength γ, taking as the starting densities the self-consistent densities from the previous γ value. There is, of course, some hysteresis involved in this process, so we do a backwards sweep on γ once we have reached the maximum interaction strength for a given run. If they differ, we use the smaller of the values obtained in upward and downward sweeps for the energy per particle. The energy per particle is obtained using the expression

$$\begin{aligned}\frac{E}{N}=&\frac{1}{\nu}\sum_{\mathbf{q}\in \mathrm{BZ}} U_{\rm dis}(\mathbf{q})\Delta_0^*(\mathbf{q})+\frac{\gamma}{2\nu}\sum_{\mathbf{q}\in \mathrm{BZ}} U_H(\mathbf{q})|\Delta_0(\mathbf{q})|^2\\&+U_F(\mathbf{q})[|\Delta_{\uparrow\uparrow}(\mathbf{q})|^2+|\Delta_{\downarrow\downarrow}(\mathbf{q})|^2+|\Delta_{\uparrow\downarrow}(\mathbf{q})|^2\\&+|\Delta_{\downarrow\uparrow}(\mathbf{q})|^2]-\frac{\gamma}{2}\tilde{g}\hat{B}\cdot\vec{P}_{\rm tot},\end{aligned}$$

where $\vec{P}_{\rm tot}$ is the total global spin polarization. The local spin magnetization density, which we calculate as well, is given by

$$\langle S_i(\mathbf{r})\rangle=\frac{\hbar}{2}\sum_{m',m,\sigma,\sigma'}\rho_{\sigma\sigma'}(x_{m'}|x_m)\tau^i_{\sigma\sigma'}\phi^*_m(\mathbf{r})\phi_{m'}(\mathbf{r}).$$

We define the local spin polarization as $\langle P_i(\mathbf{r})\rangle=2\langle S_i(\mathbf{r})\rangle/[\hbar\langle\rho(\mathbf{r})\rangle]$. Note that in this case $\langle|\vec{P}(\mathbf{r})|\rangle$ does not have to be equal to 1 since the system is compressible except in the limit of very large γ, where $\langle|\vec{P}(\mathbf{r})|\rangle\to 1$ for all $\mathbf{r}$.

Our criterion for convergence is that

$$\delta\Delta\equiv\frac{1}{N_\phi^2}\sum_{\mathbf{q}\in \mathrm{BZ}}\sum_{\sigma\sigma'}|\Delta^i_{\sigma\sigma'}(\mathbf{q})-\Delta^{i-1}_{\sigma\sigma'}(\mathbf{q})|^2<1\times10^{-6}, \tag{6}$$

where i stands for the ith iteration. We have performed calculations for several disorder realizations at different values of ν for system sizes of $N_\phi=16-32$. The finite-size effects come mainly from the effective exchange potential $U_F(\mathbf{q})$ and have been studied in detail previously.[16] The main effect is on the interaction part of the energy per particle and it is well understood and easily corrected. We believe that the physics of the phase transitions observed in these calculations is not affected qualitatively by finite-size effects. Our qualitative conclusions are based on persistent features which are obtained for several different disorder realizations. The values of γ at which the various transitions and crossovers we discuss below take place do not change by more than 5% for different realizations. The results we present here are for one particular disorder realization.

III. RESULTS AT $\nu=1$

At $\nu=1$, the disorder-free ($\gamma\to\infty$) 2DES has[1] an $S=N/2$ ground state. The $S_z=S=N/2$ member of this multiplet is a single Slater determinant and can therefore be obtained by solving Hartree-Fock equations self-consistently. It

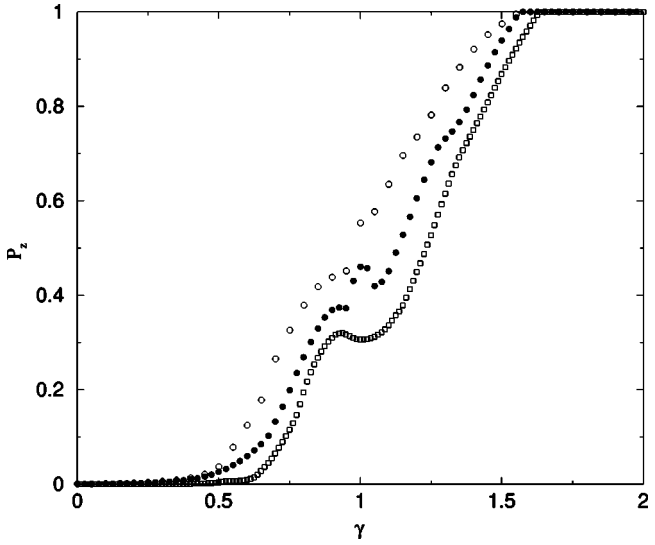

FIG. 1. Global polarization for a fixed disorder realization at $\nu=1$ with $\tilde{g}=0.015$ (filled circles) and $\tilde{g}=0.0018$ (squares). The average *magnitude* of the local polarization is shown (open circles) at $\tilde{g}=0.015$. The transition to a fully polarized state occurs at $\gamma \approx 1.6-1.9$ for all disorder realizations studied. Examples of the local polarization density and local density profile at different values of γ for a typical disorder realization are shown in Figs. 2 and 3.

is only in recent years that samples which are sufficiently clean to reach, or at least nearly reach, complete spin polarization have been grown.[5] The collective behavior producing such a ground state was not exhibited in earlier samples which had more disorder in the form of unintended impurities, interface dislocations, and, in modulation-doped samples, the potential from remote ionized donors. Figure 1 summarizes the HF theory results we have obtained for the dependence of the spin polarization on interaction strength. The calculations were performed for a realistic value of the Zeeman coupling strength, $\tilde{g}=0.015$, and at a very small value, $\tilde{g}=0.0018$. Extrapolating from these two values to $\tilde{g}=0$ allows us to identify parameter values for which spontaneous spin polarization occurs, i.e., values for which the ground state is ferromagnetic. We find that ferromagnetism occurs for $\gamma \gtrsim 0.5$ in the Hartree-Fock approximation; at smaller values of γ, the single-particle disorder term dominates and yields a spin-singlet ground state. Notice that the spin susceptibility, which may be estimated from the difference between the spin polarizations at the two $\tilde{g}$ values, is small in the singlet state, and becomes large as the phase transition to the ferromagnetic state is approached. For the specific finite-size disorder realization we have studied, complete spin polarization is reached at a finite value of $\gamma \sim 1.5$. At larger values of γ, the system has a finite gap for charge excitations. We must be aware, however, that the HF approximation overestimates the tendency of the system to order so the interaction strength at both transition points should be taken as lower limits. In addition, any physically realistic disorder potential is likely to have rare strong disorder regions which prevent the fully polarized state from being reached.

In our calculations, there is a wide region of interaction

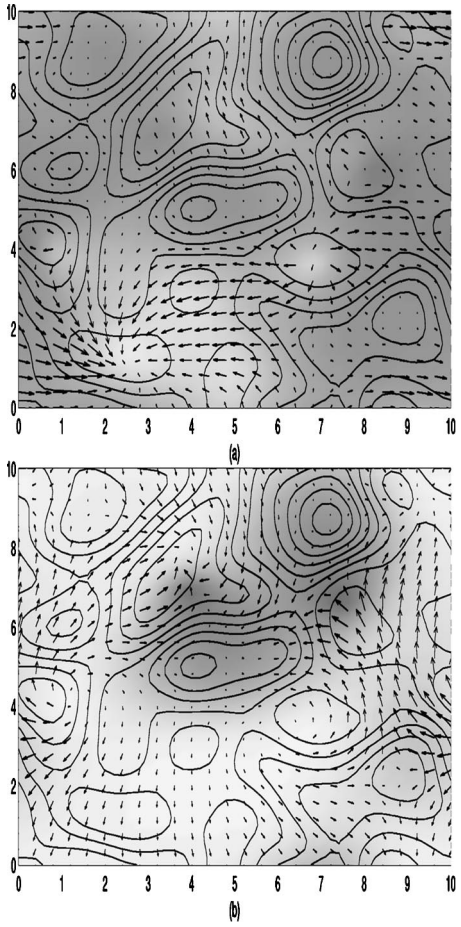

FIG. 2. Local polarization density for $\nu=1$ and $\tilde{g}=0.015$ at $\gamma=0.75$ (a) and at $\gamma=1.25$ (b). The z component is represented by a shadow plot with black as -1 and white as $+1$. The in-plane local polarization density is represented by a two-dimensional vector plot. The contour plot corresponds to the effective disorder potential used in the phase diagram shown in Fig. 1.

strengths γ for which partially spin-polarized states occur. In this regime our HF ground states nearly always have noncollinear magnetic order. We show local spin polarization and charge-density profiles of typical partially polarized states in Figs. 2 and 3. The origin of the reduced spatially integrated spin polarization is partly due to variation of spin orientation, but principally due to a reduction in the average value of the *magnitude* of the local spin polarization. This point is illustrated in Fig. 1 (open circles) and may be inferred from Fig. 2(a). The reduction in spin polarization is due to the occurrence of doubly occupied orbitals, i.e., to disorder-induced charge fluctuations which cannot be accurately described in models which include only the spin degree of freedom. The charged excitations of the ground state in this regime are ungapped and involve population of localized quasiparticle states. We also remark that local-density profiles at these relatively small γ values, illustrated in Fig. 3(a), follow the effective disorder potential smoothed by the form factor for the lowest Landau-level electrons. Rapid spatial variation components in the white noise model disorder potential have little effect on the electronic state. The relationship between electron number density and the Pontryagan index density of the local spin orientation, valid for slow spin-orientation

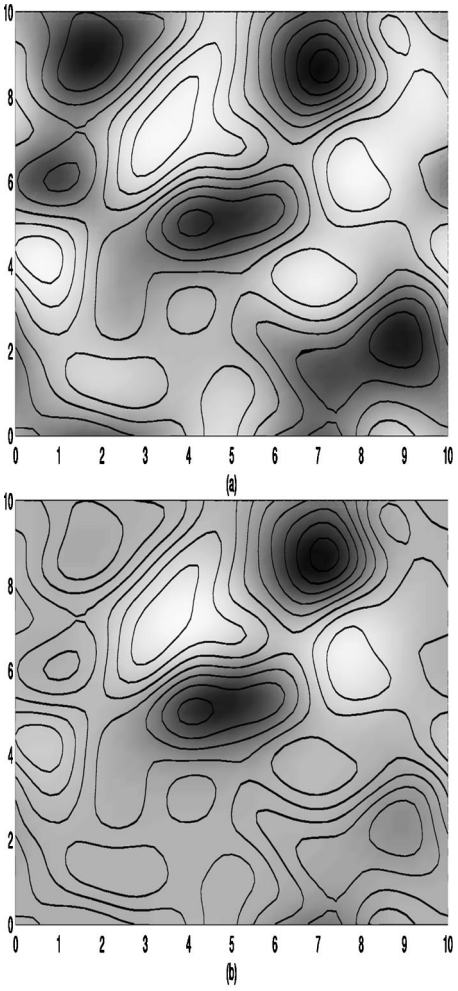

FIG. 3. Local-density profile for $\nu=1$ at $\gamma=0.75$ (a) and at $\gamma=1.25$ (b). In this shadow plot, black represents a local Landau-level filling factor of 2 and white represents a local Landau-level filling factor of zero. The contour plot corresponds to the effective disorder potential used also in the calculations of Fig. 1. Minima in the electron density occur at maxima in the effective potential and vice versa.

variation and nearly constant charge density,[1] is *not* valid in this regime. Still, the collective nature of the 2DES manifests itself in the nonzero spin-polarization density perpendicular to the Zeeman field. As interactions strengthen further, the local charge density smoothes out favoring the minimization of Coulomb energy at a cost in disorder energy. [See Figs. 2(b) and 3(b) for $\gamma\approx 1.5$.]

Experimentally, the effects of disorder can be seen most directly in the NMR spectral line shape obtained at the lowest possible temperatures where the spin profile is frozen on the experimental time scale.[12,13] The NMR intensity spectrum in this regime is given by

$$I(f,\gamma)\propto \int d\mathbf{r}\rho_N(z)e^{-(1/2\sigma^2)[2\pi f-2\pi K_s\rho_e(z)\langle\tilde{S}(\mathbf{r};\gamma)\rangle]}, \quad (7)$$

with $\sigma=9.34\ \mathrm{ms}^{-1}$ and $K_s\sim 25$ kHz. Here $\rho_N(z)$ is the nuclear polarization density and $\rho_e(z)$ is the electron density envelope function in the quantum well. The evaluation of such spectra has been outlined elsewhere;[12,13] here we simply show results for several interaction strengths in Fig. 4.

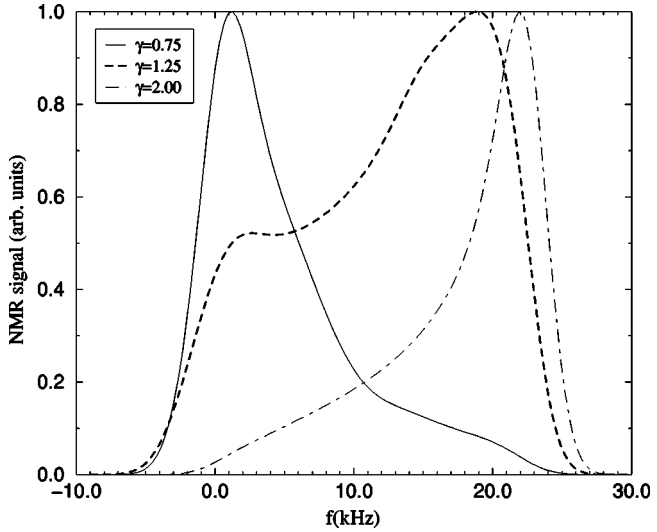

FIG. 4. NMR spectrum for $\nu=1$ and $\tilde{g}=0.015$ at $\gamma=0.75$ (solid line), at $\gamma=1.25$ (dashed thick line), and at $\gamma=2.0$ (dashed-dotted line). The sample parameters correspond to those used in the experimental studies of Ref. 13.

The parameters used in Eq. (7) are the same as the ones used in Ref. 12.

Note that the quantity usually identified experimentally as the Knight shift, the location of the peak in the NMR spectrum in Fig. 4, does not match the global polarization. This Knight shift measurement always overestimates the global polarization. In order to obtain the global polarization of the system from the measured spectrum, one has to extract the first moment of a normalized spectrum.[12] One sees from the NMR spectrum at $\gamma=1.25$ that disorder-induced spin-density variation leads to a broadening of the maximum peak and can even lead to secondary peaks at lower Knight shift frequencies. Note, however, that features corresponding to negative Knight shifts, corresponding to regions of reversed electronic spins, are unlikely because the typical size of such regions is small and because they are also obscured by the finite width of the quantum wells which trap the 2DES. Our calculations demonstrate that care must be taken in interpreting low-temperature NMR data in the quantum Hall regime.

The partially polarized regime can also be studied experimentally by measuring the transport activation gap. Provided that weak Zeeman coupling can be ignored, the extended quasiparticle states are expected to be precisely at the Fermi level when the 2DES is in a paramagnetic state. The Hall conductivity should jump from 0 to $2e^2/h$ at $\nu=1$. In the ferromagnetic state, the majority-spin extended quasiparticle state will be below the Fermi level, the majority-spin extended state will be above the Fermi level, and the Hall conductivity at $\nu=1$ should be quantized at $\sigma_{xy}=e^2/h$. The spontaneous splitting of the two extended state energies is experimentally accessible and should exhibit interesting power-law critical behavior as the ferromagnetic state is entered. This transport gap should vary monotonically with the global spin polarization, although the precise relationship between these quantities is not trivial.

It is interesting to note that the Skyrmion–anti-Skyrmion pairs predicted recently by Nederveen and Narazov[3] do not appear in our calculations. We do not conclude that these

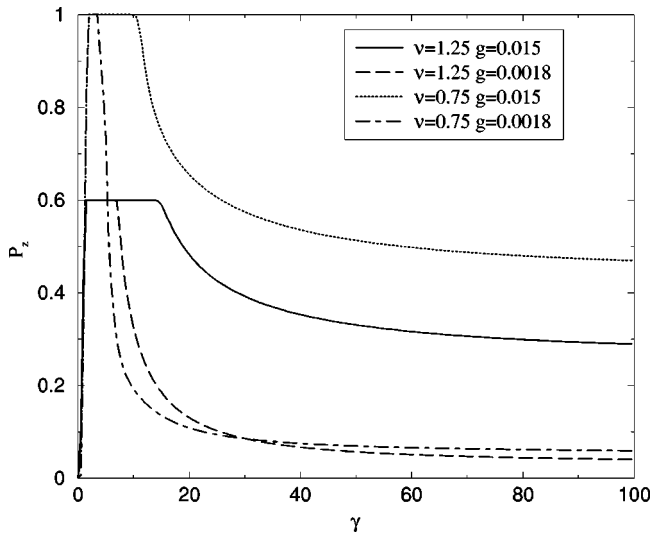

FIG. 5. Global polarization phase diagram for a fixed disorder realization at $\nu=1.25$ and $\tilde{g}=0.015$ (solid line), at $\nu=1.25$ and $\tilde{g}=0.0018$ (dashed line), at $\nu=0.75$ and $\tilde{g}=0.015$ (dotted line), and at $\nu=0.75$ and $\tilde{g}=0.0018$ (dotted-dashed line). The transition to a maximally polarized state (Laughlin quasiparticle glass) occurs at $\gamma\approx 1.5-2$ for all disorder realizations obtained. The transition from a Laughlin quasiparticle glass to a Skyrmion glass occurs at $\gamma\approx 15$ for experimentally relevant parameters. Local spin polarization density and local density at different values of γ for such disorder realization are shown in Figs. 6 and 7.

objects cannot appear at $\nu=1$; we would expect them, for example, if we choose a disorder model with relatively large potential variations, but only on a length scale much larger than the Skyrmion size. In this case the NLσ model considerations in Ref. 3 should be applicable. Our calculations demonstrate rather clearly, however, that charge-density variation at $\nu=1$ does not necessarily, or even usually, require the existence of well-defined Skyrmion quasiparticles.

IV. RESULTS AT $\nu\neq 1$

In clean (large γ) samples where full polarization is observed at $\nu=1$, the global polarization decays rapidly with $|1-\nu|$.[5] It is generally accepted that this property is a unique signature which experimentally establishes the thermodynamic stability of Skyrmion collective quasiparticles. In the strong disorder limit, on the other hand, spontaneous spin polarization does not occur at any filling factor near $\nu=1$.

The global polarization results for $\nu\neq 1$ in Fig. 5 illustrate how the system interpolates between these two extrema. As the interaction strength γ is increased from 0 to 2, the behavior is similar to the $\nu=1$ case. For strong disorder, charge variation is dominant, and small spin polarizations occur primarily because many single-particle orbitals are occupied by both up and down spin electrons. Charge variation is the dominant response to disorder, and it continues to play an important role at all interaction strengths. At sufficiently large γ, our finite-size systems reach a state with the maximum spin polarization allowed by the Pauli exclusion principle. This maximally polarized state is reached earlier than in the case at $\nu=1$ ($\gamma\sim 1.4-1.6$) because, we believe, a larger number of charged quasiparticles are available to screen the random potential. At this point the system forms what we refer to as a conventional quasiparticle glass (CQG). The conventional Laughlin quasiparticles are initially localized in the deepest minima (or maxima for $\nu<1$) of the effective disorder potential, and as the interaction strength increases, or equivalently the depth of the disorder potential wells becomes smaller, the charged quasiparticles rearrange themselves locally into a quasitriangular Wigner crystal pinned by the strongest of the disorder potential extrema. At larger γ we observe a transition from a CQG to a Skyrmion glass. The location of this transition is marked by a reduction of the global polarization from its maximally polarized value. For a specific disorder realization, the point of crossover from the CQG to the Skyrmion glass, as illustrated in Fig. 5, depends on filling factor and $\tilde{g}$. The dependence of the transition point on $\tilde{g}$ in this regime can be approximated by considering a simple model for a single Skyrmion trapped at a disorder potential extrema. We approximate its energy by

$$E(K)=U(K-K_0)^2+g^*\mu_B BK+\sigma AK, \tag{8}$$

where K is the number of spin flips per Skyrmion, σ is the strength of the disorder potential, and A is a phenomenological parameter. The first two terms determine the optimal Skyrmion size in the absence of disorder.[17] The form for the third term reflects the property that Skyrmions with smaller K are smaller and will be able to concentrate more strongly close to the potential extrema. This simple model gives an estimate of the interaction strength at which $K>0$ Skyrmions first become stable,

$$\gamma^*=\frac{A}{2K_0U/(e^2/\epsilon l)-\tilde{g}}. \tag{9}$$

The parameters U and K_0 can be estimated[17] for filling factor $\nu=1.25$ as $U/(e^2/\epsilon l)\sim 0.014$ and $K_0\sim 1$. Using our numerical result for where the transition occurs at $\tilde{g}=0.0018$, we estimate that $A\sim 0.1$. From this, one obtains an estimate of $\gamma^*\sim 7$ for the crossover point from conventional quasiparticles to Skyrmions at $\tilde{g}=0.015$. This is in reasonable agreement with the actual crossover point $\gamma^*\sim 10$ (see Fig. 5, the transition is out of scale in Fig. 8) given the simplicity of the model. These estimates of the maximum disorder strength at which Skyrmion physics is realized could be checked by performing NMR experiments in samples where electron density, and hence the interaction strength, is adjusted by the application of gate voltages.

For a particular realization of the disorder potential, particle-hole symmetry is broken in a finite system and is recovered only in the limit of very large γ. The particle-hole symmetry relation for the global spin polarization is $(1-\epsilon)P_z(\nu=1-\epsilon)=(1+\epsilon)P_z(\nu=1+\epsilon)$, where $\epsilon<1$. At large γ this relation is approximately satisfied. Also in this limit, the Pontryagan relation between the local-density profile and the local spin density[1] becomes accurate. In the clean limit, the Skyrmion system crystallizes in a square lattice for the filling factors considered here. (The Skyrmion crystal is triangular[17] for ν very close to 1.) The disordered Skyrmion glass state has very smooth fluctuations of the local spin density, compared to the CQG, although both lattices are

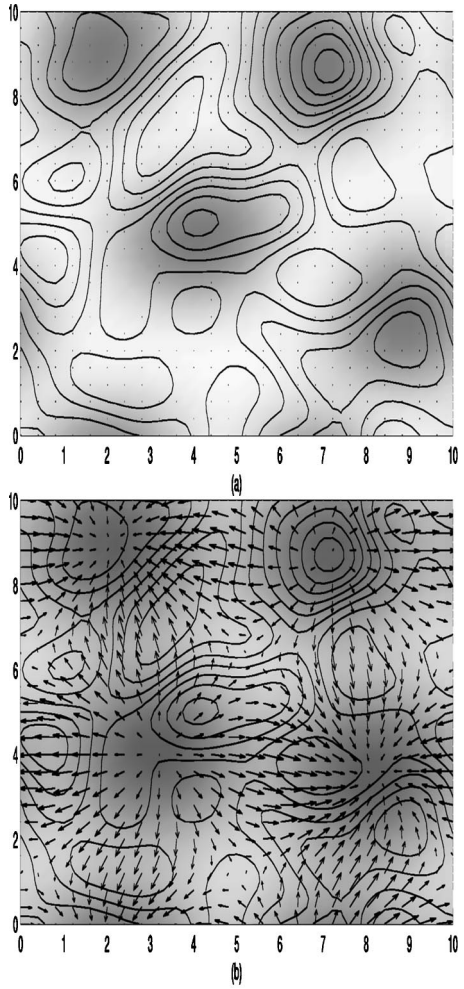

FIG. 6. Local spin-polarization density for $\nu=1.25$ at $\gamma=10.0$ (a) and at $\gamma=40.0$ (b). The z component of the spin is represented by a shadow plot with black as -1 and white as $+1$. The in-plane local spin-polarization density is represented by a two-dimensional vector plot. The contour plot shows the specific effective disorder potential which leads to these results and those illustrated in Fig. 5. Notice that spontaneous in-plane spin polarization appears only at the larger γ value.

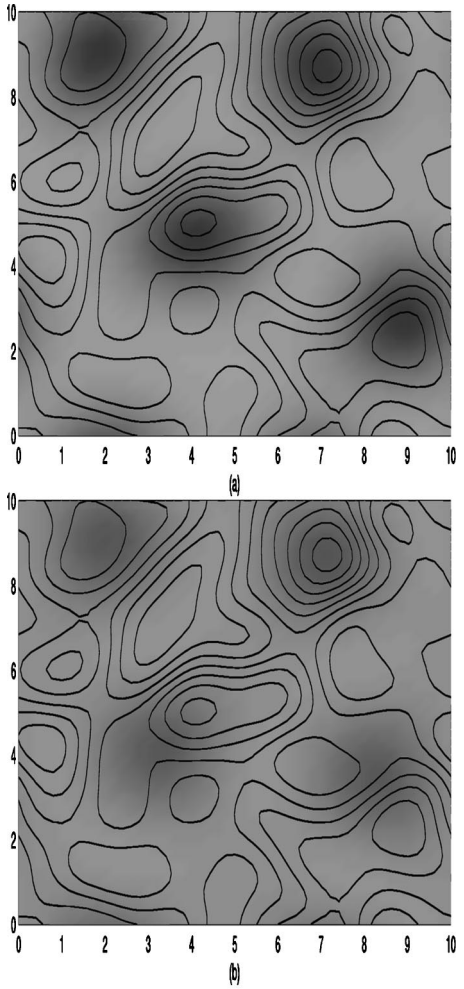

FIG. 7. Local density for $\nu=1.25$ at $\gamma=10.0$ (a) and at $\gamma=40.0$ (b). The density is represented by a shadow plot where black corresponds to local filling factor $\nu=2$ and white corresponds to local filling factor $\nu=0$. The contour plot shows the effective disorder potential used in this calculation and in Fig. 5. Notice that the density variation is smoother at larger γ when Skyrmion quasiparticles, rather than Laughlin quasiparticles, are localized near potential minima.

pinned by the disorder potential. We remark that quantum fluctuations in Skyrmion positions are not accounted for in HF theory, and it is quite possible that even in this limit the ground state is a liquid rather than a crystal.[18] As noted in Ref. 17, it is possible that the broken U(1) symmetry of the Skyrmions orientation order predicted by Hartree-Fock does not survive quantum fluctuations. We show an example of the CQG in Figs. 6(a) and 7(a), and of the quasi-Skyrmion lattice state in Figs. 6(b) and 7(b). Note that we find, in agreement with Nederveen and Narazov,[3] a shrinking of the Skyrmion size as disorder broadening increases. This effect may help explain the appearance of a ''tilted plateau'' centered around $\nu=1$ in the Knight shift vs filling factor data.[11] Rare highly disorder regions in the sample may localize and reduce the effective size of the few Skyrmions present at these filling factors. This would allow the bulk of the sample to be fully polarized at $\nu\neq 1$ and give rise to a Knight shift equivalent to the one at $\nu=1$. The plateau is tilted because of the change in fully polarized density as pointed out in Ref. 11.

V. DISCUSSION

We have used the Hartree-Fock approximation to study the competition between interactions and disorder near Landau-level filling factor $\nu=1$. At a qualitative level our results can be summarized by the schematic zero-temperature phase diagram shown in Fig. 8, which is drawn for the case of small but nonzero Zeeman coupling. Distinct ground states can be distinguished by different values for the quantized Hall conductivity, σ_{xy}, by the presence or absence of spontaneous spin polarization perpendicular to the direction of the Zeeman field, and by the presence or absence of a gap for spin-flip excitations. At small γ (strong disorder), the electronic state is paramagnetic (denoted as PC in Fig. 8), there is no spin polarization in the absence of Zeeman coupling, and the Hall conductivity is expected to jump from 0 to $2e^2/h$ as the filling factor ν crosses the $\nu=1$ line. For a small Zeeman coupling, there will be a small splitting between the majority-spin and minority-spin extended state energies, and the zero-temperature Hall conductance should

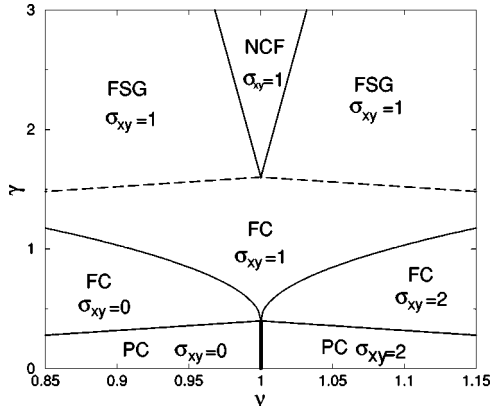

FIG. 8. Phase diagram discussed in Sec. V. Here PC indicates the compressible paramagnetic phase, FC the partially polarized compressible ferromagnetic phase, FSG the spin-gapped ferromagnetic phase, and NCF the noncollinear ferromagnetic phase. We emphasize that this phase diagram is qualitative in nature and transition points vs γ should be taken as upper limits.

have a narrow intermediate e^2/h plateau centered on $\nu=1$. However, we do not expect that this plateau will be observable at accessible temperatures, and have indicated this in Fig. 8 by using a thick line to mark the 0 to $2e^2/h$ phase boundary. At somewhat larger γ, there is a phase transition at zero Zeeman energy between paramagnetic and ferromagnetic states (denoted as FC in Fig. 8). In our calculations this transition occurs at a larger value of γ at $\nu=1$ than away from $\nu=1$. As γ increases in the ferromagnetic state, we expect that the separation between majority-spin and minority-spin extended state levels will increase rapidly so that the $\nu=1$ integer quantum Hall plateau will broaden and become observable. At still larger γ, we find a transition to a state with the maximum spin polarization allowed by the Pauli exclusion principle. At $\nu\leqslant 1$, this is full spin polarization. In these states, marked ''SG'' for spin gap in Fig. 8, the differential spin susceptibility vanishes. For realistic disorder models, it seems likely that in the thermodynamic limit there will always be rare high-disorder regions in the sample which prevent maximal spin polarization from being achieved. For this reason, the phase transition we find in our finite systems likely indicates a crossover from large to small differential spin susceptibility in macroscopic systems; we have therefore marked this transition by a dashed line. Finally at the largest values of γ (weakest disorder) the physics for ν near 1 is dominated by Skyrmion quasiparticles which emerge from the $\nu=1$ ferromagnetic vacuum. In this regime, the system develops spontaneous spin-polarization in the plane perpendicular to the direction of the Zeeman field. In Fig. 8, we have labeled this regime NCF for noncollinear ferromagnet.

This phase diagram is intended to represent the filling factor interval $0.85\leqslant\nu\leqslant 1.15$, over which fractional quantum Hall effects are not normally observed, and it appears likely that Hartree-Fock approximation calculations are able to represent interaction effects. Some of our findings may help explain the striking tilted plateau feature observed in the NMR spectra[11] near $\nu=1$. Nevertheless, we have found rich structure in the crossover between noninteracting and disorder-free limits of the $\nu=1$ quantum Hall effect, which helps explain the difficulty experienced in attempting to construct a simple interpretation of low-temperature NMR spectra. Our calculations motivate experimental studies of $\nu=1$ transport activation energy studies near the paramagnetic to ferromagnetic phase transition.

ACKNOWLEDGMENTS

Helpful conversations with S. E. Barrett, Luis Brey, and Tatsuya Nakajima are greatly appreciated. This work was supported by the National Science Foundation under Grants No. DMR-9714055 and No. DMR-9820816.

[1] For an introduction to Skyrmions and related topics, see S.M. Girvin, *The Quantum Hall Effect: Novel Excitations and Broken Symmetries*, in Les Houches Summer School 1998 (Springer Verlag and Les Editions de Physique, Paris, 1999), and references therein; S.M. Girvin and A.H. MacDonald, in *Perspectives in Quantum Hall Effects: Novel Quantum Liquids in Low-Dimensional Semiconductor Structures*, edited by S. Das Sarma and A. Pinczuk (Wiley, New York, 1997).

[2] A.G. Green, Phys. Rev. B **57**, R9373 (1998).

[3] A.J. Nederveen and Yuli V. Nazarov, Phys. Rev. Lett. **82**, 406 (1999).

[4] S.L. Sondhi, A. Karlhede, S.A. Kivelson, and E.H. Rezayi, Phys. Rev. B **47**, 16 419 (1993).

[5] R. Tycko, S.E. Barrett, G. Dabbagh, L.N. Pfeiffer, and K.W. West, Science **268**, 1460 (1995); S.E. Barrett, G. Dabbagh, L.N. Pfeiffer, K.W. West, and R. Tycko, Phys. Rev. Lett. **74**, 5112 (1995).

[6] H.A. Fertig, L. Brey, R. Côté, A.H. MacDonald, A. Karlhede, and S.L. Sondhi, Phys. Rev. B **55**, 10 671 (1997); H.A. Fertig, L. Brey, R. Côté, and A.H. MacDonald, *ibid.* **50**, 11 018 (1994).

[7] L. Brey, H.A. Fertig, R. Côté, and A.H. MacDonald, Phys. Rev. Lett. **75**, 2562 (1995).

[8] The Hartree-Fock approximation in the quantum Hall regime has been used in several earlier studies of disordered interacting systems which focus on other issues. S.-R. Eric Yang and A.H. MacDonald, Phys. Rev. Lett. **70**, 4110 (1993); S.-R. Eric Yang, A.H. MacDonald, and Bodo Huckestein, *ibid.* **74**, 3229 (1995). It has also been used in combination with a self-consistent Born approximation (SCBA) treatment of disorder which is adequate for some, but not all purposes. For a SCBA treatment of the competition between disorder and interaction driven spin-polarization, which is related to the present work, see S. Yarlagadda, Phys. Rev. B **44**, 13 101 (1991).

[9] R. Côté, A.H. MacDonald, L. Brey, H.A. Fertig, S.M. Girvin, and H.T.C. Stoof, Phys. Rev. Lett. **78**, 4825 (1997).

[10] R. Rajaraman, *Solitons and Instantons* (North-Holland, Amsterdam, 1989).

[11] S. E. Barrett, cond-mat/0009134 (unpublished).

[12] J. Sinova, S.M. Girvin, T. Jungwirth, and K. Moon, Phys. Rev. B **61**, 2749 (2000).

[13] N.N. Kuzma, P. Khandelwal, S.E. Barrett, L.N. Pfeiffer, and K.W. West, Science **281**, 686 (1998); P. Khandelwal, N.N. Kuzma, S.E. Barrett, L.N. Pfeiffer, and K.W. West, Phys. Rev. Lett. **81**, 673 (1998).

[14] Bodo Huckestein and Michael Backhaus, cond-mat/0004174 (unpublished) and references therein.

[15] F. Wegner, Z. Phys. B: Condens. Matter **51**, 279 (1983).

[16] A.H. MacDonald and G.C. Aers, Phys. Rev. B **34**, 2906 (1986).

[17] R. Côté, A.H. MacDonald, L. Brey, H.A. Fertig, S.M. Girvin, and H.T.C. Stoof, Phys. Rev. Lett. **78**, 4825 (1997).

[18] B. Paredes and J.J. Palacios, Phys. Rev. B **60**, 15 570 (1999).